Analysis of the Microstructure and Oxidation Behavior of Some Commercial Carbon Fibers

Dae Ho Kim[†], Bo-Hye Kim[†,*], Kap Seung Yang[†,‡,*], Yun Hyuk Bang[§], Sung Ryong Kim[§], and Hun Kook Im[†]

[†]*Alan G. MacDiarmid Energy Research Institute, Chonnam National University, Korea.* [*]*E-mail: ksyang@chonnam.ac.kr*
[‡]*Department of Polymer & Fiber System Engineering, Chonnam National University, Korea*
[§]*R&D Business Labs, Hyosung Corporation, Seoul, 121-720, Korea*
(Received August 4, 2011; Accepted August 7, 2011)

ABSTRACT. The relationship between the microstructure, mechanical properties, and oxidation behavior of pitch-, poly-acrylonitrile (PAN)-, and Rayon-based carbon fibers (CFs) has been studied in detail. Three types of carbon fiber were exposed to isothermal oxidation in air and the weight change was measured by thermogravimetric analyzer (TGA) apparatus. After activation energy was gained according to the conversion at reacting temperature, the value of specific surface area and the surface morphology was compared, and the reaction mechanism of oxidation affecting development of pores of carbon fibers was examined. This study will lead to a new insight into the relationship between the microstructure and mechanical properties of carbon fibers.

Key words: Carbon fiber, Microstructure, Mechanical properties, Oxidation behavior

INTRODUCTION

Carbon/carbon composites are the most promising type of fiber because of the highest specific modulus and highest specific strength of all reinforcing fibers. These properties are sustained temperatures up to higher than 2000 ºC in vacuum and inert atmospheres. However, they have low oxidation resistance in an oxidative environment (CF begins to be oxidized at 750 K in air) and chemical reactivity, and are therefore not widely used either in metal-matrix and ceramic-matrix composites or in high-temperature polymer-matrix composites.[1-3] Therefore, due to the significant influence of the oxidation behavior of CFs on the properties of the related composite materials, oxidation is one of the major limiting factors in determining the lifetime and performance of CFs and their composites in many applications.[4-6] The oxidation behavior of the composites may also be controlled by the oxidation behavior of the reinforcing fibers. Therefore, studies on the oxidation behavior of CFs have been of interest to many researchers.[7-9] The factors affecting characteristics of oxidation reaction include microstructural characteristics related to the heterogeneity taking place during the manufacturing of the carbon materials, and structural changes of pores and carbon materials by oxidation reaction.[10-13] The commercial CFs exhibit various mechanical properties, crystallite dimensions, and microstructures derived from the precursor and manu-facturing process. Therefore it will be important to observe how these parameters affect the oxidation behavior of such CFs. The present study is concentrated on the oxidation behaviors of the carbon fibers on the basis of the microstructure and the relationships with mechanical properties of the microstructure of the pitch-, PAN-, and rayon-based CFs.

EXPERIMENTAL SECTION

Materials

Characteristic properties of the CFs are presented in *Table* 1, including the manufacturers' quoted mechanical properties. A detailed study of the fiber microstructure and oxidation behavior was concentrated upon four main CFs, mesophase pitch-based CF (Pl5), PAN-based high modulus type (M40) and high tenacity types T1000 and T300, and rayon-based CF (T22). All CFs used in the study were received from commercial sources.

Oxidation

The oxidation reactions were carried out under the following conditions. The samples were heated from room temperature up to 580 ºC at a heating rate of 20 ºC/min in nitrogen flow (50 ml/min). And then samples were oxidized at 580 ºC in air flow (50 ml/min). Approximately 10 mg samples were used in each case.

Table 1. Physical and mechanical properties of the CFs

Fibers	Manufacturer	Tensile modulus (GPa)	Tensile strength (GPa)	Density (g/cm^3)	Diameter (μm)
Pitch					
P15	Kasima oil	584	2.94	2.2	7.0
PAN					
M40	Toray	377	4.40	1.75	6.0
T1000	Toray	294	6.37	1.80	6.5
T300	Toray	230	3.53	1.76	6.6
Rayon					
T22	Textiles	450	2.50	0.14	4.7

Sample characterization

Wide angle X-ray diffraction (XRD) was used to analyze the structural evolution of the CFs. XRD traces were obtained from ground-up samples of the fibers, using a D-Max-2400 diffractometer and CuKá radiation (λ=0.15418 nm). The structure of fibers was studied by using Hitachi Scanning electron microscope (SEM, S-4700, Hitachi) and compared with the structure before/after oxidation. The oxidation rates of these fibers rate were determined with the mass loss and the time reacted (air flow rate: 10 ml/min) using a thermogravimetric analyzer (TGA, Shimadzu Inc.). A heating rate of 20 ºC/min was used throughout this work. Specific surface area (SSA) and pore size distributions of the oxidized CFs were evaluated using Brunauer-Emmett-Teller (BET) equation (ASAP2020, Micromeritics, USA) after preheating the samples to 150 ºC for 2 h to eliminate the adsorbed water.

RESULTS AND DISCUSSION

Surface Morphology

Fig. 1 shows the microstructure of the surface of the various CFs before and after 50% mass loss by oxidation. On the right side in *Fig.* 1 show morphological microstructures along the perpendicular direction of various CFs partially oxidized at 50 wt.% mass loss. It was seen the development of alignment of a sheet-like layers in P15, which show parallel alignment of the grapheme-like layers at the center of the fibers as well as that towards the periphery (*Fig.* 1a). However, high strength PAN-based CFs T300 and T1000 exhibit somewhat different microstructure, which are presented to possess multi-layed microstructure in *Fig.* 1b~d. The lower crystalline regions could be etched earlier than the higher crystalline region by the oxidation reactions.[14-17] It was reported the multi-layered structure of CF caused by insufficient carbonization at the middle area of fiber during the manufacture.[18,19] The T1000 with better mechanical property exhibits more clear-cut boundary than T300. On the other hand, the high modulus
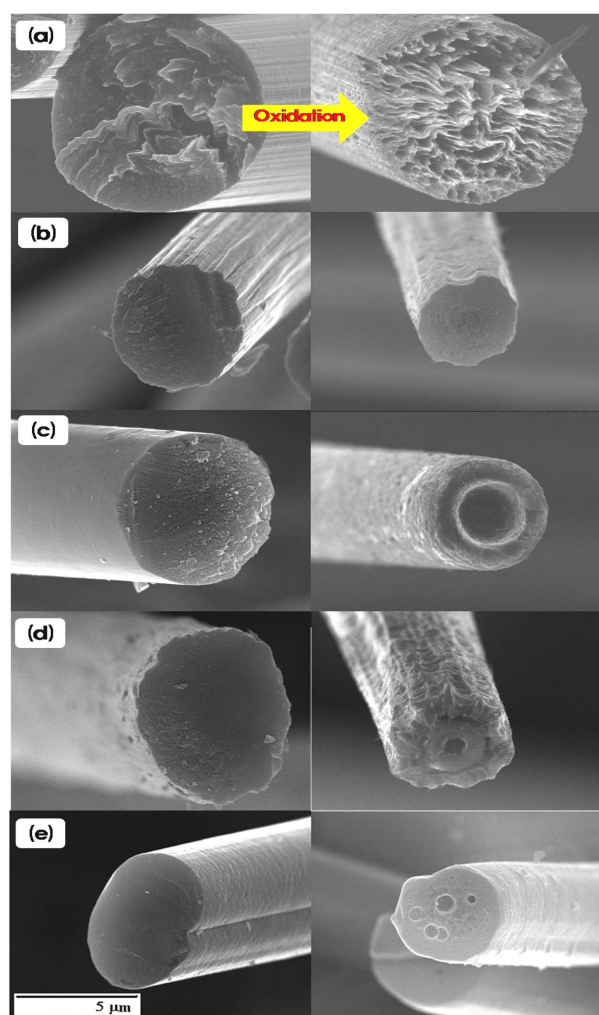

Fig. 1. SEM images of CFs of partially oxidized CFs at 50% wt.% mass loss: (a) P15 (b) M40, (c) T1000, (d) T300, (e) T22 (left side: before oxidation, right side: after oxidation).

PAN-based fiber M40 does not show any layers, which would be resulted from the homogeneously crystallization through high temperature heat treatment. The T22 formed voids all along the cross sectional area, which would be resulted from low crystalline structure in all over the fiber (*Fig.* 1e).
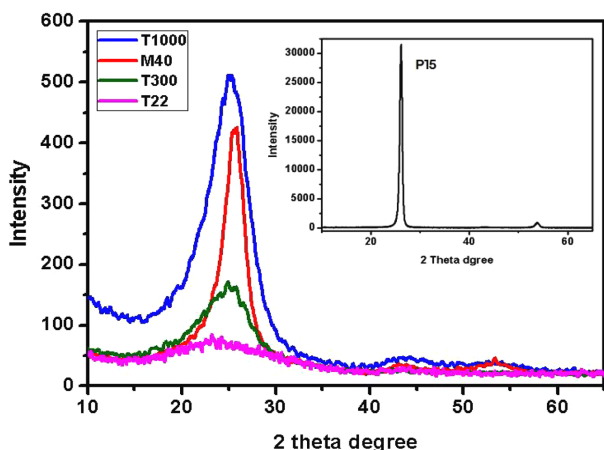
Fig. 2. X-ray diffraction spectra of various CFs.

XRD analysis

The high modulus CF shows superior mechanical, electrical and chemical properties because of its highly ordered structure. Generally, the mechanical modulus of fiber is influenced by the degree of orientation along the fiber axis.[20-22] From the XRD patterns (*Fig.* 2) of CFs except P15, broad peak located between 20 and 30° assigned as the d002 layers, representing the presence of disordered carbon structure. The (002) peak for the P15 is much sharper than any other samples, indicating the high degree of graphitization.

Apparent crystallite parameters (d002, L_c, and L_a) of various CFs as evaluated from their XRD patterns are complied in *Fig.* 3. From the position of the (002) peak (2θ) in XRD, the interplanar spacing d(002) was determined using the Bragg equation:

$$d_{(002)} = \frac{\lambda}{2\,\sin\theta_{(002)}}$$
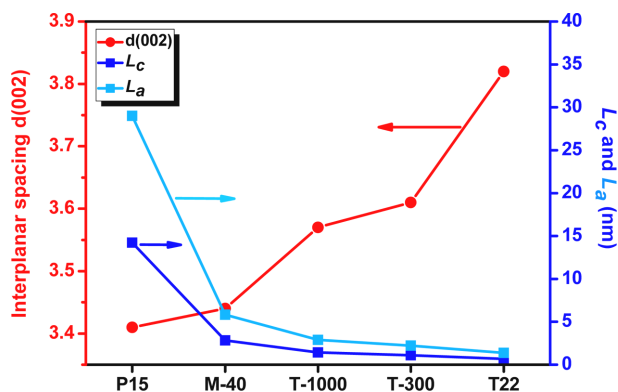
where λ is the wavelength of X-ray (0.15418 nm), and θ is

Braggs's angle. The d(002) value is traditionally used to estimate the graphitization degree of carbons. In general, growing disorder in the materials is reflected in increased values of d(002).[23] From the position and the full-width at half-maximum intensity of the (002) peak, an attempt was made to estimate the crystal size; L_c (crystalline height) and L_a (crystalline width) using the Scherrer equation:

$$L = \frac{K\lambda}{\beta\cos\theta}$$

L_c and L_a values were calculated from the peak width at half-maximum intensity, β, of the (002) peak, where $K=$ 0.9 for L_c and $K=1.84$ for L_a.[24]

As shown in *Fig.* 3, L_c and L_a values decreased, while the interlayer spacing, $d002$ value increased in the order of P15, M40, T1000, T300, T22, that is, mesophase pitch based, high modulus PAN based, high strength PAN based and rayon based. These crystallite dimensions of various CFs are in good with oxidation resistant properties of the CFs. The CFs consisted of poorly oriented crystallites and/or very tiny crystallities introduce lower activation barriers to be accessed of oxygen resulting higher rate of mass reduction by oxidation reaction because of the more porous structure.

Isothermal oxidation reaction and SSA

Fig. 4 illustrates the relation between weight loss and oxidation time when five samples were exposed to air at 853 K. It can be seen that the oxidation resistance of CFs in air increases in the order of Rayon- based (T22) < PAN-based (M40, T1000, T300) < Pitch (P15)-based CF. The rayon-based CFs with high oxidation rate reached up to 50% after oxidation for only 150 min and were almost burnt out after 200 min, while the weight loss of P15 is only 3% in 200 min. Therefore, CFs with high modulus
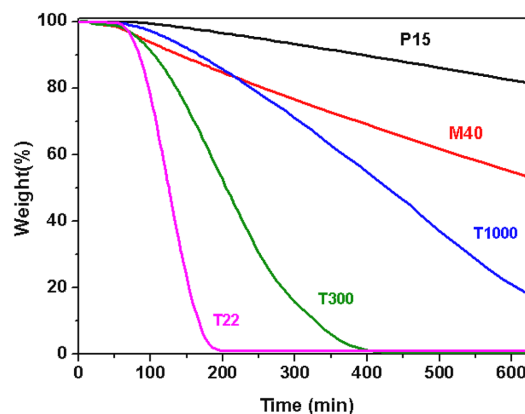

Fig. 3. The interlayer spacing d(002), crystalline height L_c and the crystalline width L_a of various CFs.

Fig. 4. TGA plots for oxidation of CFs in air at 853 K.
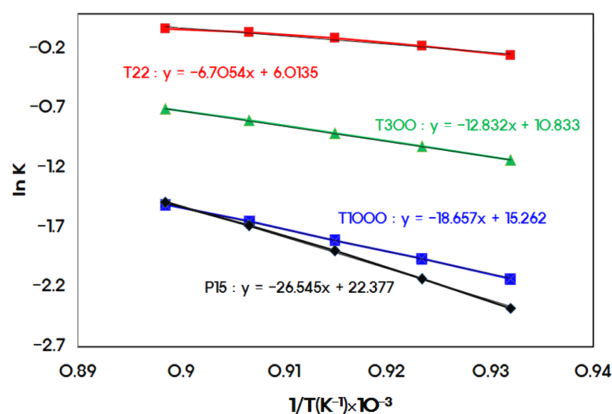
Fig. 5. Arrhenius plot of oxidation kinetics for various CFs.

Table 2. Apparent activation energies of various CFs

Fibers	Activation energy (kJ/mole)
P15	220.69
T1000	155.11
T300	106.69
T22	55.75

are found to be more oxidation resistant than CFs with high strength.

The Arrhenius curves of oxidized CFs are shown in *Fig.* 5. A plot of lnK vs. (1/T) produces the iso-conversionline and from the slope of which, the activation energy, E_a, values can be calculated at a constant conversion.[25] A plot of lnK vs. (1/T) shows good linearity and the activation energy, E_a, values can be calculated from the slope of the graph. The apparent activation energy for T22 fibers is 55.75 kJ/mole, while that of P15 fibers is 220.69 kJ/mole in *Table* 2. The reason for the difference in the reaction rates of various CFs can be explained on the basis of crystallite parameters. This means that P15 fibers have much higher crystalliity contain less edge carbon atoms (i.e., more of the initiation centers for oxidation) than other CFs.

Nitrogen adsorption measurements of the oxidized CFs (wt. loss 50%) were performed at 77 K in *Fig.* 6. According to BDDT (Brunauer-Deming-Deming-Teller) classification,[26] the isotherms are of Type I, indicating that oxidized CFs are microporous materials, and they appear to have more a rounded "knee" that is normally associated with wider micropores. It is evident that most of the pore volumes of samples are filled below $P/P_0 \approx 0.1$, indicating that these samples are highly microporous. After a sharp increase to 0.1, the isotherm slowly bends, showing smaller increments in further adsorption. Therefore, the adsorption/desorption behaviors of oxidized CFs are characterized as a typical Type I isotherm for microporous features
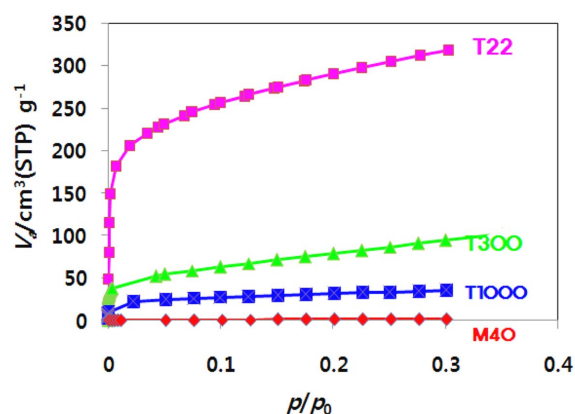

Fig. 6. Nitrogen adsorption/desorption isotherms curves of oxidized CFs (wt. loss 50%).

Table 3. The SSA values and total pore volume of oxidized CFs (wt. loss 50%)

Sample	SSA (m^2g^{-1})	Total pore volume (cm^3g^{-1})	Average pore diameter (nm)
P15	-	-	-
M40	4.6	0.003	1.79
T1000	112.4	0.055	1.94
T300	303.9	0.157	2.06
T22	1033.8	0.493	1.90

and pores well developed in oxidized in the order of P15< M40<T1000<T300<T22.

Table 3 shows the specific surface area (SSA) values and total pore volume of oxidized CFs at weight loss 50%. The oxidation reaction between reacting gas (oxygen) and carbon atoms takes place in active sites. Thus the process of pore development by oxidation reaction needs diffusion first, and then, reaction products come out through pores. As shown in *Table* 3, the oxidized M40 fibers show a very small SSA value compared T22. T1000 and T300 have high average pore diameter, due to clear-cut boundary of multi-layed microstructure in *Fig.* 1c~d. The SSA of the P15 was almost before/after oxidation. The P15 have very highly crystalline structure, and the number of active sites is limited because there is not enough space for pores to be created. In other words, the number of active sites decreases as the crystallites sizes increase. After all, oxidation reactions of the CFs are mainly dependent on defect and/or crystallinity, so there could be reasonably explained by the SSA. So, the reaction of the initial oxidation, considering the overall structure of the fiber, is likely to take place at less dense parts. The following oxidation reaction is more easily taken place after opening pores from fiber surface to inside. Since pores are created or enlarged by the removal of carbon atoms existing in the

active sites, the sizes of crystallites will decrease as the pores develop.

CONCLUSIONS

The comparative investigation of various commercial carbon fibers leads to the following results:

(a) This difference for the pitch-, PAN-, and Rayon-based CFs was explained by the relationship between microstructure, mechanical properties, and oxidation behavior.

(b) The structure of pitch-based CFs had alignment of a slit-like layers, while PAN-based CFs had the skin-core structure after oxidation.

(c) The CFs consisted of poorly oriented crystallites and/or very tiny crystallities have many crystallite edges. Since the crystallite edges will act as an active site the fiber has low oxidation resistivity.

(d) The high modulus fibers, heat treated to graphitization temperatures, were found to be more oxidation resistant than high strength carbon fibers.

REFERENCES

1. Luthra, K. L. *Carbon* **1988**, *26*, 217.
2. Baklanova, N. I.; Kulyu, V. N.; Lyakhov, N. Z. *Inorg. Mater.* **1997**, *33*, 682.
3. Kim, B.-H.; Kim, S. Y.; Kim, C.H.; Yang, K.S.; Lee, T.-J. *Appl. Surf. Sci.* **2010**, *257*, 662.
4. Prewo, K. M.; Batt, J. A. *J. Mater. Sci.* **1988**, *23*, 523.
5. Bleay, S. M.; Scott, V. D. *Carbon* **1991**, *29*, 871.
6. Cho, D.; Ha, H. S.; Lim, Y. S.; Yoon, B. I.; Kim, K. S. *Carbon* **1996**, *34*, 861.
7. Dhami, T. L.; Manocha, L. M.; Bahl, O. P. *Carbon* **1991**, *29*, 51.
8. Manocha, L. M.; Bahl, O. P. *Carbon* **1988**, *26*, 13.
9. Manocha, L. M.; Bahl, O. P.; Singh, Y. K. *Carbon* **1989**, *27*, 381.
10. Mahajan, O. P.; Yarzab, R.; Walker, P. L. *Fuel* **1978**, *57*, 643.
11. Sanchez, A. R.; Elguezabal, A. A.; Torre Saenz, L. L. *Carbon* **2001**, *39*, 1367.
12. Kasaoka, S.; Sakata, Y.; Kayano, S.; Masuoka, Y. *Int. Chem. Eng.* **1983**, *23*, 477.
13. Hu, Y. Q.; Nikzat, H.; Nawata, M.; Kobayashi, N.; Hasatani, M. *Fuel* **2001**, *80*, 2111.
14. Matsumoto, T.; Mochida, I. *Carbon* **1993**, *31*, 143.
15. Blanco, C.; Lu, S. *Carbon* **2003**, *41*, 165.
16. Warner, S. B.; Peebles, L. H.; Uhlmann, D. R. *J. Mater. Sci.* **1979**, *14*, 556.
17. Lv, M.-Y.; Ge, H.-Y.; Chen, J. J. *Polym. Res.* **2008**, *16*, 513.
18. Blanco, S.; Lu, C.; Rand, B. *Carbon* **2002**, *40*, 132.
19. Roh, J.-S.; Kim, S.-H. *Carbon Lett.* **2009**, *10*, 38.
20. Donnet, J. B.; Bansal, R. C. *Carbon Fibers*, 2nd ed.; Marcel Decker: New York, 1990.
21. Dami, T. L.; Manocha, L. M.; Bahl, O. P. *Carbon* **1999**, *29*, 51.
22. Ismail, M. K. *Carbon* **1991**, *29*, 777.
23. Liu, C.-L.; Dong, W.-S.; Song, J.-R.; Liu, L. *Mater. Sci. Eng. A* **2007**, *459*, 347.
24. Cullity, B. D. *Elements of X-Ray Diffraction*; Addison-Wesley Publishing Company: Menlo Park, 1978.
25. Gao, P.; Wang, H.; Jin, Z. *Thermochimica. Acta* **2004**, *414*, 59.
26. Brunauer, B.; Deming, L. S.; Deming, W. E.; Teller, E. *J. Am. Chem. Soc.* **1940**, *62*, 1723.